1

One Dimensional Turbulent Transfer Using Random Square Waves – Scalar/Velocity and Velocity/Velocity Interactions

H. E. Schulz[1,2], G. B. Lopes Júnior[2], A. L. A. Simões[2] and R. J. Lobosco[2]
[1]*Nucleus of Thermal Engineering and Fluids*
[2]*Department of Hydraulics and Sanitary Engineering School of Engineering of São Carlos, University of São Paulo*
Brazil

1. Introduction

The mathematical treatment of phenomena that oscillate randomly in space and time, generating the so called "statistical governing equations", is still a difficult task for scientists and engineers. Turbulence in fluids is an example of such phenomena, which has great influence on the transport of physical proprieties by the fluids, but which statistical quantification is still strongly based on *ad hoc* models. In turbulent flows, parameters like velocity, temperature and mass concentration oscillate continuously in turbulent fluids, but their detailed behavior, considering all the possible time and space scales, has been considered difficult to be reproduced mathematically since the very beginning of the studies on turbulence. So, statistical equations were proposed and refined by several authors, aiming to describe the evolution of the "mean values" of the different parameters (see a description, for example, in Monin & Yaglom, 1979, 1981).

The governing equations of fluid motion are nonlinear. This characteristic imposes that the classical statistical description of turbulence, in which the oscillating parameters are separated into mean functions and fluctuations, produces new unknown parameters when applied on the original equations. The generation of new variables is known as the "closure problem of statistical turbulence" and, in fact, appears in any phenomena of physical nature that oscillates randomly and whose representation is expressed by nonlinear conservation equations. The closure problem is described in many texts, like Hinze (1959), Monin & Yaglom (1979, 1981), and Pope (2000), and a general form to overcome this difficulty is matter of many studies.

As reported by Schulz et al. (2011a), considering scalar transport in turbulent fluids, an early attempt to theoretically predict RMS profiles of the concentration fluctuations using "ideal random signals" was proposed by Schulz (1985) and Schulz & Schulz (1991). The authors used random square waves to represent concentration oscillations during mass transfer across the air-water interface, and showed that the RMS profile of the concentration fluctuations may be expressed as a function of the mean concentration profile. In other words, the mean concentration profile helps to know the RMS profile. In these studies, the authors did not consider the effect of diffusion, but argued that their

equation furnished an upper limit for the normalized RMS value, which is not reached when diffusion is taken into account.
The random square waves were also used by Schulz et al. (1991) to quantify the so called "intensity of segregation" in the superficial boundary layer formed during mass transport, for which the explanations of segregation scales found in Brodkey (1967) were used. The time constant of the intensity of segregation, as defined in the classical studies of Corrsin (1957, 1964), was used to correlate the mass transfer coefficient across the water surface with more usual parameters, like the Schmidt number and the energy dissipation rate. Random square waves were also applied by Janzen (2006), who used the techniques of Particle Image Velocimetry (PIV) and Laser Induced Fluorescence (LIF) to study the mass transfer at the air-water interface, and compared his measurements with the predictions of Schulz & Schulz (1991) employing *ad hoc* concentration profiles. Further, Schulz & Janzen (2009) confirmed the upper limit for the normalized RMS of the concentration fluctuations by taking into account the effect of diffusion, also evaluating the thickness of diffusive layers and the role of diffusive and turbulent transports in boundary layers. A more detailed theoretical relationship for the RMS of the concentration fluctuation showed that several different statistical profiles of turbulent mass transfer may be interrelated.
Intending to present the methodology in a more organized manner, Schulz et al. (2011a) showed a way to "model" the records of velocity and mass concentration (that is, to represent them in an *a priori* simplified form) for a problem of mass transport at gas-liquid interfaces. The fluctuations of these variables were expressed through the so called "partition, reduction, and superposition functions", which were defined to simplify the oscillating records. As a consequence, a finite number of basic parameters was used to express all the statistical quantities of the equations of the problem in question. The extension of this approximation to different Transport Phenomena equations is demonstrated in the present study, in which the mentioned statistical functions are derived for general scalar transport (called here "scalar-velocity interactions"). A first application for velocity fields is also shown (called here "velocity-velocity interactions"). A useful consequence of this methodology is that it allows to "close" the turbulence equations, because the number of equations is bounded by the number of basic parameters used. In this chapter we show 1) the *a priori* modeling (simplified representation) of the records of turbulent variables, presenting the basic definitions used in the random square wave approximation (following Schulz et al., 2011a); 2) the generation of the usual statistical quantities considering the random square wave approximation (scalar-velocity interactions); 3) the application of the methodology to a one-dimensional scalar transport problem, generating a closed set of equations easy to be solved with simple numerical resources; and 4) the extension of the study of Schulz & Johannes (2009) to velocity fields (velocity-velocity interactions).
Because the method considers primarily the oscillatory records itself (*a priori* analysis), and not phenomenological aspects related to physical peculiarities (*a posteriori* analysis, like the definition of a turbulent viscosity and the use of turbulent kinetic energy and its dissipation rate), it is applicable to any phenomenon with oscillatory characteristics.

2. Scalar-velocity interactions

2.1 Governing equations for transport of scalars: Unclosed statistical set

The turbulent transfer equations for a scalar F are usually expressed as

$$\frac{\partial \overline{\mathrm{F}}}{\partial \mathrm{t}} + \overline{\mathrm{V}}_{\mathrm{i}} \frac{\partial \overline{\mathrm{F}}}{\partial \mathrm{x}_{\mathrm{i}}} = \frac{\partial}{\partial \mathrm{x}_{\mathrm{i}}} \left(\mathrm{D}_{\mathrm{F}} \frac{\partial \overline{\mathrm{F}}}{\partial \mathrm{x}_{\mathrm{i}}} - \overline{\mathrm{v}_{\mathrm{i}} \mathrm{f}} \right) + \overline{\mathrm{g}} \text{ , } i = 1, 2, 3. \tag{1}$$

where $\overline{F}$ and f are the mean scalar function and the scalar fluctuation, respectively. $\overline{V_i}$ (i = 1, 2, 3) are mean velocities and v_i are velocity fluctuations, t is the time, x_i are the Cartesian coordinates, $\overline{g}$ represents the scalar sources and sinks and D_F is the diffusivity coefficient of F. For one-dimensional transfer, without mean movements and generation/consumption of F, equation (1) with $x_3=z$ and $v_3=\omega$ is simplified to

$$\frac{\partial \overline{\mathrm{F}}}{\partial \mathrm{t}} = \frac{\partial}{\partial \mathrm{z}} \left(\mathrm{D}_{\mathrm{F}} \frac{\partial \overline{\mathrm{F}}}{\partial \mathrm{z}} - \overline{\omega \mathrm{f}} \right) \tag{2}$$

As can be seen, a second variable, given by the mean product $\overline{\omega f}$, is added to the equation of $\overline{F}$, so that a second equation involving $\overline{\omega f}$ and $\overline{F}$ is needed to obtain solutions for both variables. Additional statistical equations may be generated averaging the product between equation (1) and the instantaneous fluctuations elevated to some power (f^{θ}). As any new equation adds new unknown statistical products to the problem, the resulting system is never closed, so that no complete solution is obtained following strictly statistical procedures (closure problem). Studies on turbulence consider a low number of statistical equations (involving only the first statistical moments), together with additional equations based on *ad hoc* models that close the systems. This procedure seems to be the most natural choice, because having already obtained equation (2), it remains to model the new parcel $\overline{\omega f}$ *a posteriori* (that is, introducing hypotheses and definitions to solve it). An example is the combined use of the Boussinesq hypothesis (in which the turbulent viscosity/diffusivity is defined) with the Komogoroff reasoning about the relevance of the turbulent kinetic energy and its dissipation rate. The $\kappa - \varepsilon$ model for statistical turbulence is then obtained, for which two new statistical equations are generated, one of them for k and the other for ε. Of course, new unknown parameters appear, but also additional *ad hoc* considerations are made, relating them to already defined variables.

In the present chapter, as done by Schulz et al. (2011a), we do not limit the number of statistical equations based on *a posteriori* definitions for $\overline{\omega f}$. Convenient *a priori* definitions are used on the oscillatory records, obtaining transformed equations for equation (1) and additional equations. The central moments of the scalar fluctuations, $\overline{f^{\theta}} = \overline{\left[F - \overline{F} \right]^{\theta}}$, θ= 1, 2, 3,… are considered here. For example, the one-dimensional equations for θ=2, 3 and 4, are given by

$$\frac{1}{2} \frac{\partial \overline{f^2}}{\partial t} + \overline{f\omega} \frac{\partial \overline{F}}{\partial z} + \frac{1}{2} \frac{\partial \overline{f^2 \omega}}{\partial z} = D_F \left(\overline{f \frac{\partial^2 f}{\partial z^2}} \right) \tag{3a}$$

$$\frac{1}{3} \frac{\partial \overline{f^3}}{\partial t} + \overline{f^2} \frac{\partial \overline{F}}{\partial t} + \overline{f^2 \omega} \frac{\partial \overline{F}}{\partial z} + \frac{1}{3} \frac{\partial \overline{\omega f^3}}{\partial z} = D_F \left(\overline{f^2 \frac{\partial^2 \overline{F}}{\partial z^2}} + \overline{f^2 \frac{\partial^2 f}{\partial z^2}} \right) \tag{3b}$$

$$\frac{1}{4}\frac{\partial \overline{f^4}}{\partial t}+\overline{f^3}\frac{\partial \overline{F}}{\partial t}+\overline{f^3\omega}\frac{\partial \overline{F}}{\partial z}+\frac{1}{4}\frac{\partial \overline{\omega f^4}}{\partial z}=D_F\left(\overline{f^3}\frac{\partial^2\overline{F}}{\partial z^2}+\overline{f^3\frac{\partial^2 f}{\partial z^2}}\right) \tag{3c}$$

In this example, equation (3a) involves $\overline{F}$ and $\overline{f\omega}$ of equation (2), but adds three new unknowns. The first four equations (2) and (3 a, b, c) already involve eleven different statistical quantities: $\overline{F}$, $\overline{f^2}$, $\overline{f^3}$, $\overline{f^4}$, $\overline{f\omega}$, $\overline{f^2\omega}$, $\overline{f^3\omega}$, $\overline{f^4\omega}$, $\overline{f\frac{\partial^2 f}{\partial z^2}}$, $\overline{f^2\frac{\partial^2 f}{\partial z^2}}$, and $\overline{f^3\frac{\partial^2 f}{\partial z^2}}$, and the "closure" is not possible. The general equation for central moments, for any θ, is given by [20]

$$\frac{1}{\theta}\frac{\partial \overline{f^\theta}}{\partial t}+\overline{f^{\theta-1}}\frac{\partial \overline{F}}{\partial t}+\overline{f^{\theta-1}\omega}\frac{\partial \overline{F}}{\partial z}+\frac{1}{\theta}\frac{\partial \overline{\omega f^\theta}}{\partial z}=D_F\left(\overline{f^{\theta-1}}\frac{\partial^2\overline{F}}{\partial z^2}+\overline{f^{\theta-1}\frac{\partial^2 f}{\partial z^2}}\right) \tag{3d}$$

(using θ=1 reproduces equation (2)).
As mentioned, the method models the records of the oscillatory variables, using random square waves. The number of equations is limited by the number of the basic parameters defined "*a priori*".

2.2 "Modeling" the records of the oscillatory variables

As mentioned in the introduction, the term "modeling" is used here as "representing in a simplified way". Following Schulz et al. (2011a), consider the function $F(z, t)$ shown in Figure 1. It represents a region of a turbulent fluid in which the scalar quantity F oscillates between two functions F_p (p=previous) and F_n (n=next) in the interval $z_1<z<z_2$. Turbulence is assumed stationary.

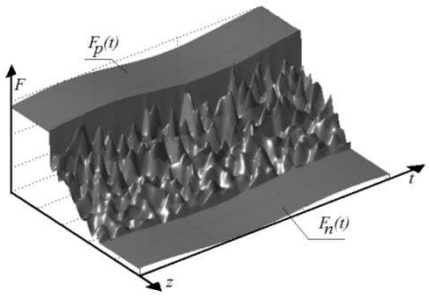

Fig. 1a. A two-dimensional random scalar field F oscillating between the boundary functions F_p(t) and F_n(t).

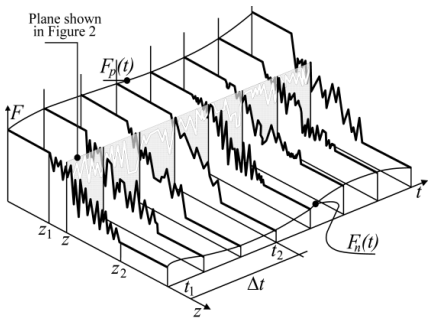

Fig. 1b. Sketch of the region shown in figure (1a). Turbulence is stationary. Adapted from Schulz et al. (2011a)

The time average of $F(z, t)$ for $z_1 < z < z_2$, indicated by $\overline{F}(z,t)$ is defined as usual

$$\overline{F}(z,t)=\frac{1}{\Delta t}\int_{t_1}^{t_2}F(z,t)dt \qquad for \qquad z_1<z<z_2 \tag{4}$$

$\Delta t = t_2 - t_1$ is the time interval for the average operation. Equation (4) generates a mean value $\overline{F}(z)$ for $z_1 < z < z_2$ and $t_1 < t < t_2$. Any statistical quantity present in equations 3, like, for example, the central moments $\overline{f^\theta} = \overline{\left[F - \overline{F}\right]^\theta}$, is defined according to equation (4). To simplify notation, both coordinates (z, t) are dropped off in the rest of the text.
The method described in the next sections allows to obtain the relevant statistical quantities of the governing equations, like the mean function $\overline{F}$, using simplified records of F.

2.3 Bimodal square wave: Mean values using a time-partition function for the scalar field - *n*

The basic assumptions made to "model" the original oscillatory records may be followed considering Figure 2. In this sense, figure 2a is a sketch of the original record of the scalar variable F at a position $z_1 < z < z_2$, as shown in the gray vertical plane of Figure 1. The objective of this analysis is to obtain an equation for the mean function $\overline{F}(z)$ for $t_1 < t < t_2$, which is also shown in figure 2a. The values of the scalar variable during the turbulent transfer are affected by both the advective turbulent movements and diffusion. Discarding diffusion, the value of F would ideally alternate between the limits F_p and F_n (the bimodal square wave), as shown in Figure 2b (the fluid particles would transport only the two mentioned F values). This condition was assumed as a first simplification, but maintaining the correct mean, in which $\overline{F}(z)$ is unchanged. It is known that diffusion induces fluxes governed by F differences between two regions of the fluid (like the Fourier law for heat transfer and the Fick law for mass transfer). These fluxes may significantly lower the amplitude of the oscillations in small patches of fluid, and are taken into account using F_p-P and F_n+N for the two new limiting F values, as shown in Figure 2c. The parcels P and N depend on z.
In other words, the amplitude of the square oscillations is "adjusted" (modeled), in order to approximate it to the mean amplitude of the original record. As can be seen, the aim of the method is not only to evaluate $\overline{F}$ adequately, but also the lower order statistical quantities that depend on the fluctuations, which are relevant to close the statistical equations. The parcels P and N were introduced based on diffusion effects, but any cause that inhibits oscillations justifies these corrective parcels.
The first statistical parameter is represented by n, and is defined as the fraction of the time for which the system is at each of the two F values (equations 5 and 6), being thus named as "partition function". This function n depends on z and is mathematically defined as

$$n = \frac{t \text{ at } (F_p - P)}{\Delta t \text{ of the observation}} \tag{5}$$

This definition also implies that

$$1 - n = \frac{t \text{ at } (F_n + N)}{\Delta t \text{ of the observation}} \tag{6}$$

$\overline{F}$ remains the same in figures 2a, b and c. The constancy between figures 2b and c is obtained using mass conservation, implying that P and N are related through equation (7):

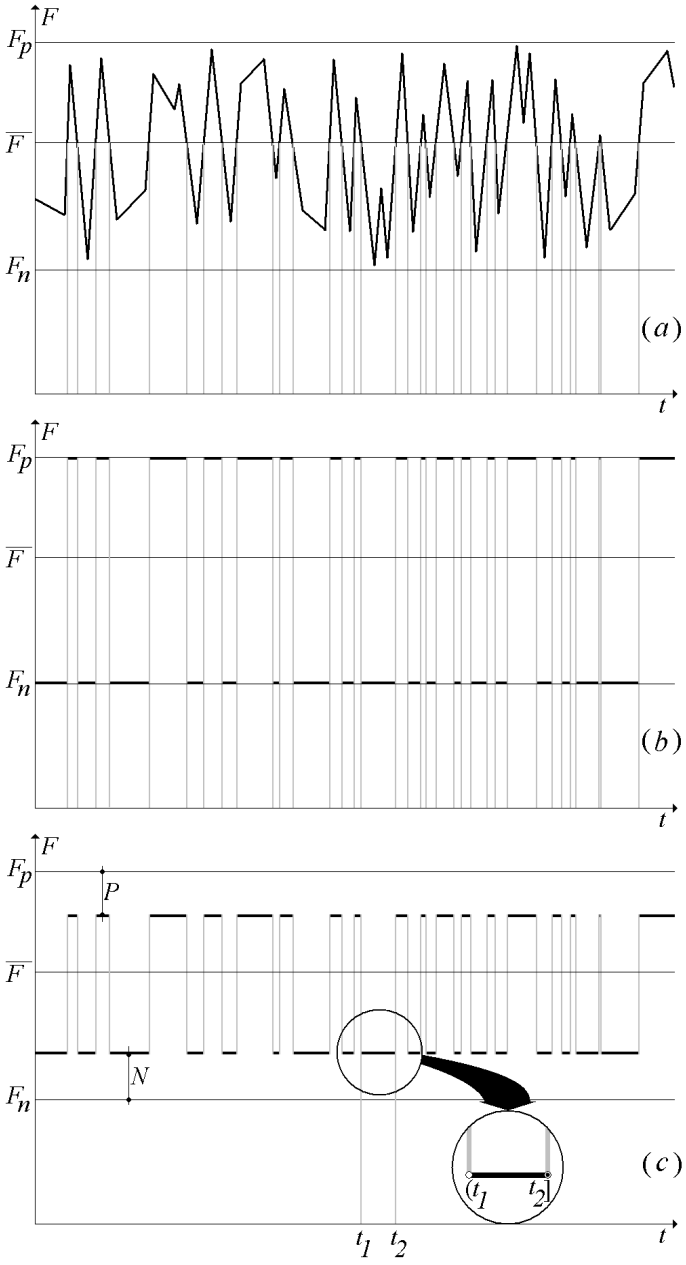

Fig. 2. *a*) Sketch of the *F* record of the gray plane of figure 1, at *z*, *b*) Simplified record alternating *F* between F_p and F_n, *c*) Simplified record with amplitude damping. Upper and lower points do not superpose at the discontinuities (the *F* segments are open at the left and closed at the right, as shown in the detail).

$$N = \frac{P\,n}{(1-n)} \tag{7}$$

The mean value of F is obtained from a weighted average operation between F_p-P and F_n+N, using equations (5) through (7). It follows that

$$\overline{F} = n\,F_p + (1-n)\,F_n \tag{8}$$

Isolating n, equation (8) leads to

$$n = \frac{\overline{F} - F_n}{F_p - F_n} \tag{9}$$

Thus, the partition function n previously defined by equation (5) coincides with the normalized form of $\overline{F}$ given by equation (9). Note that n is used as weighting factor for any statistical parameter that depends on F. For example, the mean value $\overline{Q}$ of a function $Q(F)$ is calculated similarly to equation (8), furnishing

$$\overline{Q} = n\,Q\left(F_p - P\right) + (1-n)\,Q\left(F_n + N\right) \tag{9a}$$

As a consequence, equations (9) and (9a) show that any new mean function $\overline{Q}$ is related to the mean function $\overline{F}$. Or, in other words: because n is used to calculate the different mean profiles, all profiles are interrelated.
From the above discussion it may be inferred that any new variable added to the problem will have its own partition function. In the present section of scalar-velocity interactions, two partition functions are described: n for F (scalar) and m for V (velocity).

2.4 Bimodal square wave: Adjusting amplitudes using a reduction coefficient function for scalars - α_f

The sketch of figure 2c shows that the parcel P is always smaller or equal to $F_p - \overline{F}$. As already mentioned, this parcel shows that the amplitude of the fluctuations is reduced. Thus, a reduction coefficient α_f is defined here as

$$P = \alpha_f \left[F_p - \overline{F}\right] \qquad 0 \le \alpha_f \le 1 \tag{10}$$

where α_f is a function of z and quantifies the reduction of the amplitude due to interactions between parcels of liquid with different F values (described here as a measure of diffusion effects, but which can be a measure of any cause that inhibits fluctuations). Using the effect of diffusion to interpret the new function, values of α_f close to 1 or 0 indicate strong or weak influence of diffusion, respectively. Considering this interpretation, Schulz & Janzen (2009) reported experimental profiles for α_f in the mass concentration boundary layer during air-water interfacial mass-transfer, which showed values close to 1 in both the vicinity of the surface and in the bulk liquid, and closer to 0 in an intermediate region (giving therefore a minimum value in this region).

From equations (7), (8) and (10), N and P are now expressed as

$$\left.\begin{aligned} N &= \alpha_f\, n\left(F_p - F_n\right) \\ P &= \alpha_f \left(1-n\right)\left(F_p - F_n\right) \end{aligned}\right\} \qquad 0 \le \alpha_f \le 1 \tag{11}$$

As for the partition functions, any new variable implies in a new reduction coefficient. In the present section of scalar-velocity interactions, only the reduction coefficient for F is used (that is, α_f). In the section for velocity-velocity interactions, a reduction coefficient α_v for V (velocity) is used.

2.5 Bimodal square wave: Quantifying superposition using the superposition coefficient function - β

Let us now consider the two main variables of turbulent scalar transport, the scalar F and the velocity V, oscillating simultaneously in the interval $z_1<z<z_2$ of Figure 1. As usual, they are represented as $F = \overline{F} + f$ and $V = \overline{V} + \omega$, where $\overline{F}$ and $\overline{V}$ are the mean values, and f and ω are the fluctuations. The correlation coefficient function $\rho(z)$ for the fluctuations f and ω is given by

$$\rho(z) = \frac{1}{\Delta t}\int_{t_1}^{t_2} \rho(z,t)\,dt = \frac{1}{\Delta t}\int_{t_1}^{t_2} \frac{\omega f}{\sqrt{\overline{\omega^2}}\sqrt{\overline{f^2}}}\,dt = \frac{\overline{\omega f}}{\sqrt{\overline{\omega^2}}\sqrt{\overline{f^2}}} \tag{12}$$

If the fluctuations are generated by the same cause, it is expected that the records of ω and f are at least partially superposed. As done for F, it is assumed that the oscillations ω can be positive or negative and so a partition function m (a function of z) may be defined. If we consider a perfect superposition between f and ω, it would imply in n=m, though this is not usually the case. Aiming to consider all the cases, a superposition coefficient β is defined so that β=1.0 reflects the direct superposition (m=n), and β=0.0 implies the inverse superposition of the positive and the negative fluctuations (m=1-n) of both fields.

The definition of β is better understood considering the scheme presented in figure 3. In this figure all positive fluctuations of the scalar variable were put together, so that the nondimensional time intervals were added, furnishing the value n. As a consequence, the nondimensional fraction of time of the juxtaposed negative fluctuations appears as 1-n. The velocity fluctuations also appear juxtaposed, showing that β=1 superposes f and n with the same sign (++ and --), while β=0 superposes f and n with opposite signs (+- and -+). The positive and negative scalar fluctuations are represented by f_1 and f_2, respectively. The downwards and upwards velocity fluctuations are represented by ω_d and ω_u, respectively.

Thus, m, which defines the fraction of the time for which the system is at ω_d, is expressed as

$$m = 1 - \left(\beta + n - 2\beta n\right) \tag{13}$$

β is a function of z. Also here any new variable implies in new superposition functions. In the present section of scalar-velocity interactions only one superposition coefficient function is used (linking scalar and velocity fluctuations).

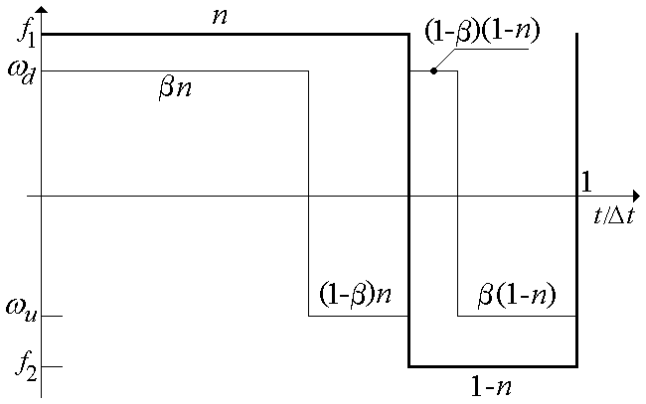

Fig. 3. Juxtaposed fluctuations of f and ω, showing a compact form of the time fractions n and $(1-n)$, and the use of the superposition function β. The horizontal axis represents the time as shown in equations (5) and (6).

2.6 The fluctuations around the mean for bimodal square waves

An advantage of using random square waves as shown in Figure 2 is that they generate only two fluctuation amplitudes for each variable, which are then used to calculate the wished statistical quantities. Of course, the functions defined in sections 2.3 through 2.5 (partition, reduction and superposition functions) are also used, and they must "adjust" the statistical quantities to adequate values. From equations (8), (10), and (11), the two instantaneous scalar fluctuations are then given by equations (14) and (15)

$$f_1 = \left(F_p - P - \overline{F}\right) = (1-n)\left(F_p - F_n\right)\left(1-\alpha_f\right) \quad \text{(positive)} \tag{14}$$

$$f_2 = \left(F_n + N - \overline{F}\right) = -n\left(F_p - F_n\right)\left(1-\alpha_f\right) \quad \text{(negative)} \tag{15}$$

2.7 Velocity fluctuations and the RMS velocity

In figure 1 the scalar variable is represented oscillating between two homogeneous values. But nothing was said about the velocity field that interacts with the scalar field. It may also be bounded by homogeneous velocity values, but may as well have zero mean velocities in the entire physical domain, without any evident reference velocity. This is the case, for example, of the problem of interfacial mass transfer across gas-liquid interfaces, the application shown by Schulz et al. (2011a). In such situations, it is more useful to use the rms velocity $\sqrt{\overline{\omega^2}}$ as reference, as commonly adopted in turbulence. For the one-dimensional case, with null mean motion, all equations must be derived using only the vertical velocity fluctuations ω. It is necessary, thus, to obtain equations for $\sqrt{\overline{\omega^2}}$ and for the velocity fluctuations (like equations 14 and 15 for f) considering the random square waves approximation. An auxiliary velocity scale U is firstly defined, shown in figure 4, considering "downwards" (ω_d) and "upwards" (ω_u) fluctuations, which amplitudes are functions of z.

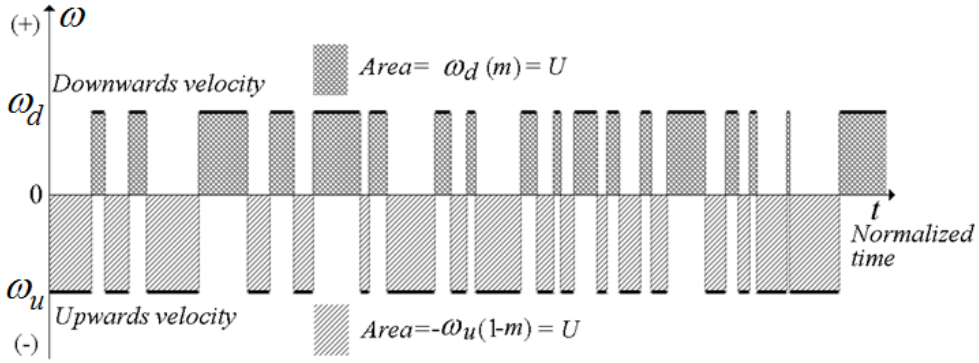

Fig. 4. The definition of the partition function m and the velocity scale U. Upwards (-) and downwards (+) velocities are shown. The dark and light gray areas are equal, so that the mean velocity is zero.

Using m for the partition function of the velocity, the scale U shown in figure 4 is defined as the integration of the upper or the lower parts of the graph in Figure 4, as

$$U = \omega_d m \qquad \text{and} \qquad U = -\omega_u (1-m) \tag{16}$$

Equation (17) describes the zero mean velocity (remembering that ω_u is negative)

$$\omega_d m + \omega_u (1-m) = 0 \qquad \text{or} \qquad U - U = 0 \tag{17}$$

U is a function of z. Let us now consider the RMS velocity $\sqrt{\overline{\omega^2}}$, which is calculated as

$$\overline{\omega^2} = m\omega_d^2 + (1-m)(-\omega_u)^2 \qquad \text{and} \qquad \sqrt{\overline{\omega^2}} = \sqrt{m\omega_d^2 + (1-m)(-\omega_u)^2} \tag{18}$$

U and $\sqrt{\overline{\omega^2}}$ may be easily related. From equations (13), (16), and (18) it follows that

$$U = \sqrt{\overline{\omega^2}} \sqrt{\left[1-(\beta+n-2\beta n)\right](\beta+n-2\beta n)} \tag{19}$$

Finally, the velocity fluctuations may be related to $\sqrt{\overline{\omega^2}}$, n and β using equations (16) and (19)

$$\omega_d = \sqrt{\overline{\omega^2}} \sqrt{\frac{\beta+n-2\beta n}{1-(\beta+n-2\beta n)}} \qquad \text{and} \qquad \omega_u = -\sqrt{\overline{\omega^2}} \sqrt{\frac{1-(\beta+n-2\beta n)}{\beta+n-2\beta n}} \tag{20}$$

$\sqrt{\overline{\omega^2}}$ is a function of z and is used as basic parameter for situations in which no evident reference velocities are present. For the example of interfacial mass transfer, $\sqrt{\overline{\omega^2}}$ is zero at the water surface (z=0) and constant ($\neq 0$) in the bulk liquid ($z \to \infty$).

The basic functions n, α_f, β, $\sqrt{\overline{\omega^2}}$, defined in items 2.3 through 2.7, are used in the sequence to calculate the statistical quantities of the one-dimensional equations for scalar-velocity interactions. Further, incorporating them into equations (2) and (3), a closed set of equations for these functions is generated. In other words, the one dimensional turbulent transport problem reduces to the calculation of these functions, defined *a priori* to their inclusion in the equations. Some of their general characteristics are described in table 1.
The RMS velocity may be normalized to be also bounded by the (absolute) values of 0.0 and 1.0. Because the position of the maximum value depends on the situation under study, needing more detailed explanations, the table is presented with the RMS velocity in dimensional form and having an undetermined maximum value.

Function	n	α_f	β	$\sqrt{\overline{\omega^2}}$
Dimension	Nondimensional	Nondimensional	Nondimensional	Velocity
Physical ground	Partition	Reduction	Superposition	Ref. velocity
Maximum value	1	1	1	Undetermined
Minimum value	0	0	0	0

Table 1. Characteristics of the functions defined for one dimensional scalar transport.

A further conclusion is that, because four functions need to be calculated, it implies that only four equations must be transformed to the random square waves representation in this one-dimensional situation. As a consequence, only lower order statistical quantities present in these equations need to be transformed, which is a positive consequence of this approximation, because the simplifications (and associated deviations) will not be propagated to the much higher order terms (they will not be present in the set of equations).

2.8 The central moments of scalar quantities using random square waves

It was shown that equations (3) involve central moments like $\overline{f^2}$, $\overline{f^3}$, $\overline{f^4}$, which, as mentioned, must be converted to the square waves representation. The general form of the central moments is defined as

$$\overline{f^\theta} = \overline{\left[F - \overline{F}\right]^\theta} \qquad \theta = 1,2,3,... \tag{21}$$

For any statistical phenomenon, the first order central moment (θ=1) is always zero. Using equations (14) and (15), Schulz & Janzen (2009) showed that the second order central moment ($\overline{f^2}$ for θ=2) is given by

$$\overline{f^2} = f_1^{\,2} n + f_2^{\,2}(1-n) = n(1-n)\left(1-\alpha_f\right)^2\left(F_p - F_n\right)^2 \tag{22}$$

or, normalizing the RMS value (f'_2)

$$f'_2 = \frac{\sqrt{\overline{f^2}}}{\left(F_p - F_n\right)} = \sqrt{n(1-n)}\left(1-\alpha_f\right) \qquad \alpha_f = 1 - \frac{\sqrt{\overline{f^2}}}{\left(F_p - F_n\right)\sqrt{n(1-n)}} \tag{23}$$

This form is useful to obtain the reduction function α_f from experimental data, using the normalized mean profile and the RMS profile, as shown by Schulz & Janzen (2009). Equation (23) shows that diffusion, or other causes that inhibit the fluctuations and imply in $\alpha_f \neq 0$, imposes a peak of f'_2 lower than 0.5.

The general central moments (θ=1, 2, 3…) for the scalar fluctuation f are given by

$$\overline{f^\theta} = f_1{}^\theta n + f_2{}^\theta (1-n) = n(1-n)\left[(1-n)^{\theta-1} + (-1)^\theta (n)^{\theta-1}\right]\left(F_p - F_n\right)^\theta \left(1-\alpha_f\right)^\theta \tag{24}$$

or, normalizing the θ^{th} root (f_θ)

$$f'_\theta = \frac{\sqrt[\theta]{\overline{f^\theta}}}{\left(F_p - F_n\right)} = \sqrt[\theta]{n(1-n)\left[(1-n)^{\theta-1} + (-1)^\theta (n)^{\theta-1}\right]}\left(1-\alpha_f\right) \tag{25}$$

The functional form of the statistical quantities shown here must be obtained solving the transformed turbulent transport equations (that is, the equations involving these quantities). Equations (21) through (25) show that, given n and α_f, it is possible to calculate all the central moments ($\overline{f^\theta}$ statistical profiles) needed in the one-dimensional equations for scalar transfer.

2.9 The covariances and correlation coefficient functions using random square waves

2.9.1 The turbulent flux of the scalar $\dot{F}$

The turbulent scalar flux, denoted by $\dot{F}$, is defined as the mean product between scalar fluctuations (f) and velocity fluctuations (ω)

$$\dot{F} = \overline{\omega f} \tag{26}$$

Thus $\overline{\omega f}$ in equation (2) is the turbulent flux of F along z. The statistical correlation between ω and f is given by the correlation coefficient function, r, defined as

$$r = \frac{\overline{\omega f}}{\sqrt{\overline{\omega^2}}\sqrt{\overline{f^2}}} \tag{27}$$

r is a function of z, and $0 \leq |r| \leq 1$. As it is clear from equations (26) and (27), r is also the normalized turbulent flux of F and reaches a peak amplitude less than or equal to 1.0, a range convenient for the present method, coinciding with the defined functions n, α_f, β, also bounded by 0.0 and 1.0 (as shown in table 1). The present method allows to express r as dependent on n, the normalized mean profile of F.

2.9.2 The correlation coefficient functions $\overline{f^\theta \omega}$

Equations (3) involve turbulent fluxes like $\overline{f\omega}$, $\overline{f^2\omega}$, $\overline{f^3\omega}$, $\overline{f^4\omega}$, which are unknown variables that must be expressed as functions of n, α_f, β and $\sqrt{\overline{\omega^2}}$. For products between any power of f and ω, the superposition coefficient β must be used to account for an "imperfect" superposition between the scalar and the velocity fluctuations. Therefore the flux $\overline{\omega f}$ is calculated as shown in equation (28), with β being equally applied for the positive and negative fluctuations, as shown in figure 3

$$\overline{\omega f} = \omega_d\left[f_1 n\beta + f_2(1-n)(1-\beta)\right] + \omega_u\left[f_1 n(1-\beta) + f_2(1-n)\beta\right] \tag{28}$$

Equations (13) through (20) and (28) lead to

$$\overline{\omega f} = \sqrt{\overline{\omega^2}}\left(F_p - F_n\right)\left(1-\alpha_f\right)(1-n)n(2\beta-1)\left\{\sqrt{\frac{\beta+n-2\beta n}{1-(\beta+n-2\beta n)}} + \sqrt{\frac{1-(\beta+n-2\beta n)}{\beta+n-2\beta n}}\right\} \tag{29}$$

Rearranging, the turbulent scalar flux is expressed as

$$\overline{\omega f} = \frac{n(1-n)\left(1-\alpha_f\right)\sqrt{\overline{\omega^2}}\left(F_p - F_n\right)}{\sqrt{n(1-n) + \dfrac{\beta(1-\beta)}{(2\beta-1)^2}}} \tag{30}$$

Equations (23), (27) and (30) lead to the correlation coefficient function

$$r\big|_{\omega,f} = \frac{\overline{\omega f}}{\sqrt{\overline{\omega^2}}\sqrt{\overline{f^2}}} = \sqrt{\frac{n(1-n)}{n(1-n) + \dfrac{\beta(1-\beta)}{(2\beta-1)^2}}} \qquad \text{with} \qquad 0 \le \left| r\big|_{\omega,f} \right| \le 1 \tag{31}$$

Schulz el al. (2010) used this equation together with data measured by Janzen (2006). The "ideal" turbulent mass flux at gas-liquid interfaces was presented (perfect superposition of f and ω, obtained for β = 1.0). Is this case, $r\big|_{\omega,f} = 1$, and $\overline{\omega f} = \sqrt{\overline{\omega^2}}\sqrt{\overline{f^2}}$. The measured peak of $\sqrt{\overline{\omega^2}}$, represented by W, was used to normalize $\overline{\omega f}$, as shown in Figure 5.
Considering r as defined by equation (27), it is now a function of n and β only. Generalizing for f^θ, we have

$$\overline{\omega f^\theta} = \omega_d\left[f_1^\theta n\beta + f_2^\theta(1-n)(1-\beta)\right] + \omega_u\left[f_1^\theta n(1-\beta) + f_2^\theta(1-n)\beta\right] \tag{32}$$

The correlation coefficient function is now given by

$$r\big|_{\omega,f^\theta} = \frac{\overline{\omega f^\theta}}{\sqrt{\overline{f^{2\theta}}}\sqrt{\overline{\omega^2}}} = \sqrt{\frac{n(1-n)}{n(1-n) + \dfrac{\beta(1-\beta)}{(2\beta-1)^2}}}\left\{\frac{\left[(1-n)^\theta - (-n)^\theta\right]}{\sqrt{\left[(1-n)^{2\theta-1} + (-1)^{2\theta}(n)^{2\theta-1}\right]}}\right\} \tag{33}$$

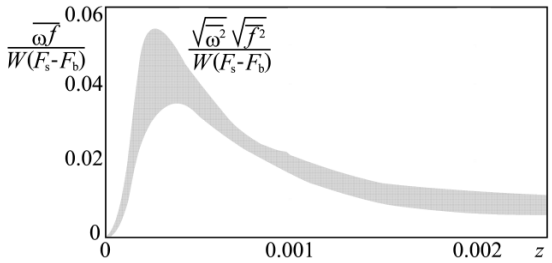

Fig. 5. Normalized "ideal" turbulent fluxes for β=1 using measured data. W is the measured peak of $\sqrt{\overline{\omega^2}}$. z is the vertical distance from the interface. Adapted from Schulz et al. (2011a).

Equation (32) is used to calculate covariances like $\overline{f^2\omega}$, $\overline{f^3\omega}$, $\overline{f^4\omega}$, present in equations (3). For example, for θ=2, 3 and 4 the normalized fluxes are given, respectively, by:

$$r\big|_{\omega,f^2} = \frac{\overline{\omega f^2}}{\sqrt{\overline{f^4}}\sqrt{\overline{\omega^2}}} = \sqrt{\frac{n(1-n)}{n(1-n)+\dfrac{\beta(1-\beta)}{(2\beta-1)^2}}}\left\{\frac{(1-2n)}{\sqrt{\left[(1-n)^3+(n)^3\right]}}\right\} \tag{34a}$$

$$r\big|_{\omega,f^3} = \frac{\overline{\omega f^3}}{\sqrt{\overline{f^6}}\sqrt{\overline{\omega^2}}} = \sqrt{\frac{n(1-n)}{n(1-n)+\dfrac{\beta(1-\beta)}{(2\beta-1)^2}}}\left\{\frac{\left[(1-n)^3+n^3\right]}{\sqrt{\left[(1-n)^5+(n)^5\right]}}\right\} \tag{34b}$$

$$r\big|_{\omega,f4} = \frac{\overline{\omega f^4}}{\sqrt{\overline{f^8}}\sqrt{\overline{\omega^2}}} = \sqrt{\frac{n(1-n)}{n(1-n)+\dfrac{\beta(1-\beta)}{(2\beta-1)^2}}}\left\{\frac{\left[(1-n)^4-n^4\right]}{\sqrt{\left[(1-n)^7+(n)^7\right]}}\right\} \tag{34c}$$

As an ideal case, for β=1 (perfect superposition) equation 33 furnishes

$$r\big|_{\omega,f^\theta} = \frac{\overline{\omega f^\theta}}{\sqrt{\overline{f^{2\theta}}}\sqrt{\overline{\omega^2}}} = \left\{\frac{\left[(1-n)^\theta-(-n)^\theta\right]}{\sqrt{\left[(1-n)^{2\theta-1}+(-1)^{2\theta}(n)^{2\theta-1}\right]}}\right\} \tag{35}$$

and the normalized covariances $\overline{f^2\omega}$, $\overline{f^3\omega}$, $\overline{f^4\omega}$, for θ=2, 3 and 4, are then given, respectively, by:

$$r\big|_{\omega,f^2} = \left\{\frac{(1-2n)}{\sqrt{\left[(1-n)^3+(n)^3\right]}}\right\} \tag{36a}$$

$$r\big|_{\omega,f^3} = \left\{ \frac{\left[(1-n)^3 + n^3 \right]}{\sqrt{\left[(1-n)^5 + (n)^5 \right]}} \right\} \tag{36b}$$

$$r\big|_{\omega,f4} = \left\{ \frac{\left[(1-n)^4 - n^4 \right]}{\sqrt{\left[(1-n)^7 + (n)^7 \right]}} \right\} \tag{36c}$$

Equations (34a) and (36a) can be used to analyze the general behavior of the flux $\overline{f^2\omega}$. These equations involve the factor $(1-2n)$, which shows that this flux changes its direction at n=0.5. For 0<n<0.5 the flux $\overline{f^2\omega}$ is positive, while for 0.5<n<1.0, it is negative. In the mentioned example of gas-liquid mass transfer, the positive sign indicates a flux entering into the bulk liquid, while the negative sign indicates a flux leaving the bulk liquid. This behavior of $\overline{f^2\omega}$ was described by Magnaudet & Calmet (2006) based on results obtained from numerical simulations. A similar change of direction is observed for the flux $\overline{f^4\omega}$, easily analyzed through the polynomial $(1-n)^4 - n^4$.

The equations of items 2.9.1 and 2.9.2 confirm that the normalized turbulent fluxes are expressed as functions of n and β only, while the covariances may be expressed as functions of n, β, α_f and $\sqrt{\overline{\omega^2}}$.

2.10 Transforming the derivatives of the statistical equations

2.10.1 Simple derivatives

The governing differential equations (2) and (3) involve the derivatives of several mean quantities. The different physical situations may involve different physical principles and boundary conditions, so that "particular" solutions may be found. For the example of interfacial mass transfer reported in the cited literature (e.g. Wilhelm & Gulliver, 1991; Jähne & Monahan, 1995; Donelan, et al., 2002; Janzen et al., 2010, 2011), F_p is taken as the constant saturation concentration of gas at the gas-liquid interface, and F_n is the homogeneous bulk liquid gas concentration. In this chapter this mass transfer problem is considered as example, because it involves an interesting definition of the time derivative of F_n.

The p^{th}-order space derivative $\frac{\partial^p \overline{F}}{\partial z^p}$ is obtained directly from equation (8), and is given by

$$\frac{\partial^p \overline{F}}{\partial z^p} = \left(F_p - F_n \right) \frac{\partial^p n}{\partial z^p} \tag{37}$$

The time derivative of the mean concentration, $\frac{\partial \overline{F}}{\partial t}$, is also obtained from equation (8) and eventual previous knowledge about the time evolution of F_p and F_n. For interfacial mass transfer the time evolution of the mass concentration in the bulk liquid follows equation (38) (Wilhelm & Gulliver, 1991; Jähne & Monahan, 1995; Donelan, et al., 2002; Janzen et al., 2010, 2011)

$$\frac{dF_n}{dt} = K_f\left(F_p - F_n\right) \tag{38}$$

This equation applies to the boundary value F_n or, in other words, it expresses the time variation of the boundary condition F_n shown in figure 1. K_f is the transfer coefficient of F (mass transfer coefficient in the example). To obtain the time derivative of $\overline{F}$, equations (8) and (38) are used, thus involving the partition function n. In this example, n depends on the agitation conditions of the liquid phase, which are maintained constant along the time (stationary turbulence). As a consequence, n is also constant in time. The time derivative of $\overline{F}$ in equation (8) is then given by

$$\frac{\partial \overline{F}}{\partial t} = \frac{\partial\left[n F_p + (1-n)F_n\right]}{\partial t} = (1-n)\frac{\partial F_n}{\partial t} \tag{39}$$

From equations (38) and (39), it follows that

$$\frac{\partial \overline{F}}{\partial t} = K_f(1-n)\left(F_p - F_n\right) \tag{40}$$

Equation (40) is valid for boundary conditions given by equation (38) (usual in interfacial mass and heat transfers). As already stressed, different physical situations may conduce to different equations.

The time derivatives of the central moments $\overline{f^\theta}$ are obtained from equation (24), furnishing:

$$\frac{\partial \overline{f^\theta}}{\partial t} = -\theta n(1-n)\left[(1-n)^{\theta-1} + (-1)^\theta (n)^{\theta-1}\right]\left(F_p - F_n\right)^{\theta-1}\left(1-\alpha_f\right)^\theta \frac{\partial F_n}{\partial t}$$

or (41)

$$\frac{\partial \overline{f^\theta}}{\partial t} = -\theta K n(1-n)\left[(1-n)^{\theta-1} + (-1)^\theta (n)^{\theta-1}\right]\left(F_p - F_n\right)^\theta \left(1-\alpha_f\right)^\theta$$

As no velocity fluctuation is involved, only the partition function n is needed to obtain the mean values of the derivatives of $\overline{f^\theta}$, that is, no superposition coefficient is needed. The obtained equations depend only on n and α_f, the basic functions related to F.

2.10.2 Mean products between powers of the scalar fluctuations and their derivatives

Finaly, the last "kind" of statistical quantities existing in equations (3) involve mean products of fluctuations and their second order derivatives, like $\overline{f\frac{\partial^2 f}{\partial z^2}}$, $\overline{f^2\frac{\partial^2 f}{\partial z^2}}$, and $\overline{f^3\frac{\partial^2 f}{\partial z^2}}$. The general form of such mean products is given in the sequence. From equations (14) and (15), it follows that

$$f_1^\theta \frac{\partial^2 f_1}{\partial z^2} = \left[(1-n)\left(F_p - F_n\right)\left(1-\alpha_f\right)\right]^\theta \frac{\partial^2\left[(1-n)\left(1-\alpha_f\right)\right]}{\partial z^2}\left(F_p - F_n\right) \tag{42}$$

$$f_2^{\theta}\frac{\partial^2 f_2}{\partial z^2}=\left[-n\left(F_p-F_n\right)\left(1-\alpha_f\right)\right]^{\theta}\frac{\partial^2\left[-n\left(1-\alpha_f\right)\right]}{\partial z^2}\left(F_p-F_n\right) \tag{43}$$

Using the partition function n, we obtain the mean product

$$\overline{f^{\theta}\frac{\partial^2 f}{\partial z^2}}=\left\{(1-n)^{\theta-1}\frac{\partial^2\left[(1-n)\left(1-\alpha_f\right)\right]}{\partial z^2}+(-n)^{\theta-1}\frac{\partial^2\left[-n\left(1-\alpha_f\right)\right]}{\partial z^2}\right\}n(1-n)\left(1-\alpha_f\right)^{\theta}\left(F_p-F_n\right)^{\theta+1} \tag{44}$$

Equation (44) shows that mean products between powers of f and its derivatives are expressed as functions of n and α_f only.

2.11 The heat/mass transport example

In this section, the simplified example presented by Schulz et al. (2011a) is considered in more detail. The simplified condition was obtained by using a constant α_f, in the range from 0.0 to 1.0. The obtained differential equations are nonlinear, but it was possible to reduce the set of equations to only one equation, solvable using mathematical tables like Microsoft Excel® or similar.

2.11.1 Obtaining the transformed equations for the one-dimensional transport of F

Equation (2) may be transformed to its random square waves correspondent using equations (2), (8), (30), (37), and (40), leading to

$$K_f\left(1-n\right)=D_f\frac{d^2n}{dz^2}-\frac{d}{dz}\left\{\frac{n(1-n)\left(1-\alpha_f\right)\sqrt{\overline{\omega^2}}}{\sqrt{n(1-n)+\frac{\beta(1-\beta)}{(2\beta-1)^2}}}\right\} \tag{45}$$

In the same way, equation (3d) is transformed to its random square waves correspondent using equations (3d), (8), (24), (32), (37), (41), and (44), leading to

$$\begin{aligned}
&-K_f\,n(1-n)\left[(1-n)^{\theta-1}+(-1)^{\theta}(n)^{\theta-1}\right]\left(1-\alpha_f\right)^{\theta}+\\
&+K_f n(1-n)^2\left[(1-n)^{\theta-2}+(-1)^{\theta-1}(n)^{\theta-2}\right]\left(1-\alpha_f\right)^{\theta-1}+\\
&+\sqrt{\frac{\left[n(1-n)\right]^{3-\theta}}{n(1-n)+\frac{\beta(1-\beta)}{(2\beta-1)^2}}}\left[(1-n)^{\theta-1}-(-n)^{\theta-1}\right]\left[n(1-n)\right]^{(\theta-1)/2}\sqrt{\overline{\omega^2}}\left(1-\alpha_f\right)^{\theta-1}\frac{\partial n}{\partial z}+\\
&+\frac{1}{\theta}\frac{\partial}{\partial z}\left\{\sqrt{\frac{\left[n(1-n)\right]^{2-\theta}}{n(1-n)+\frac{\beta(1-\beta)}{(2\beta-1)^2}}}\left[(1-n)^{\theta}-(-n)^{\theta}\right]\left[n(1-n)\left(1-\alpha_f\right)^2\right]^{\theta/2}\sqrt{\overline{\omega^2}}\right\}=
\end{aligned}$$

$$= D_f\, n(1-n)\left[(1-n)^{\theta-2} + (-1)^{\theta-1}(n)^{\theta-2}\right]\left(1-\alpha_f\right)^{\theta-1}\frac{\partial^2 n}{\partial z^2} +$$

$$+D_f\left\{(1-n)^{\theta-2}\frac{\partial^2\left[(1-n)\left(1-\alpha_f\right)\right]}{\partial z^2} + (-n)^{\theta-2}\frac{\partial^2\left[-n\left(1-\alpha_f\right)\right]}{\partial z^2}\right\} n(1-n)\left(1-\alpha_f\right)^{\theta-1} \qquad (46)$$

2.11.2 Simplified case of interfacial heat/mass transfer

Although involving few equations for the present case, the set of the coupled nonlinear equations (45) and (46) may have no simple solution. As mentioned, the original one-dimensional problem needs four equations. But as the simplified solution of interfacial transfer using a mean constant $\alpha_f = \overline{\alpha_f}$ is considered here, only three equations would be needed. Further, recognizing in equations (45) and (46) that β and $\sqrt{\overline{\omega^2}}$ appear always together in the form

$$IJ = \frac{n(1-n)\left(1-\alpha_f\right)\sqrt{\overline{\omega^2}}}{\sqrt{n(1-n)+\dfrac{\beta(1-\beta)}{(2\beta-1)^2}}} \qquad (47)$$

It is possible to reduce the problem to a set of only two coupled equations, for n and the function IJ. Thus, only equations (45) and (46) for θ=2 are necessary to close the problem when using $\alpha_f = \overline{\alpha_f}$. Defining $A = (1-\overline{\alpha_f})$ the set of the two equations is given by

$$K_f(1-n) = D_f\frac{d^2n}{dz^2} - \frac{d(IJ)}{dz} \qquad (48a)$$

$$-K_f\, n(1-n)A^2 + (IJ)\frac{dn}{dz} + \frac{A}{2}\frac{d}{dz}\left[(IJ)(1-2n)\right] = -2D_f\, n(1-n)A^2\frac{d^2n}{dz^2} \qquad (48b)$$

Equations (48) may be presented in nondimensional form, using $z^*=z/E$, with $E=z_2-z_1$, and $S=1/\kappa=D_f/K_fE^2$

$$IJ^* = \frac{n(1-n)\left(1-\alpha_f\right)\left(\sqrt{\overline{\omega^2}}/KE\right)}{\sqrt{n(1-n)+\dfrac{\beta(1-\beta)}{(2\beta-1)^2}}} \qquad (49)$$

$$(1-n) = S\frac{d^2n}{dz^{*2}} - \frac{d(IJ^*)}{dz^*} \qquad (50a)$$

$$-n(1-n)A^2 + (IJ^*)\frac{dn}{dz^*} + \frac{A}{2}\frac{d}{dz^*}\left[(IJ^*)(1-2n)\right] = -2Sn(1-n)A^2\frac{d^2n}{dz^{*2}} \qquad (50b)$$

Equation (50a) is used to obtain dIJ/dz^*, which leads, when substituted into equation (50b), to the following governing equation for n (see appendix 1)

$$\begin{aligned}
&A\left[2An(1-n)+\frac{(1-2n)}{2}\right]\frac{d^3n}{dz^{*3}}\frac{dn}{dz^*}+\\
&+A\left\{-\left[2An(1-n)+\frac{(1-2n)}{2}\right]\frac{d^2n}{dz^{*2}}+\kappa(1-n)\left[\frac{2n(A-1)+1}{2}\right]+\frac{\left\{1+2A\left[A(1-2n)-1\right]\right\}}{A}\left(\frac{dn}{dz^*}\right)^2\right\}\frac{d^2n}{dz^{*2}}+\\
&+\kappa\left\{(A-1)(1-n)-A\left[A(1-2n)-\left(\frac{3}{2}-2n\right)\right]\right\}\left(\frac{dn}{dz^*}\right)^2=0
\end{aligned} \tag{51}$$

Thus, the one-dimensional problem is reduced to solve equation (51) alone. It admits non-trivial analytical solution for the extreme case A=0 (or $\overline{\alpha_f}=1$), in the form

$$\frac{d^2n}{dz^{*2}}=\kappa(1-n) \qquad \text{or} \qquad n=1-\frac{\sin\left(\sqrt{\kappa}z^*\right)}{\sin\left(\sqrt{\kappa}\right)} \tag{52}$$

But this effect of diffusion for all $0<z^*<1$ is considered overestimated. Equation (51) was presented by Schulz et al. (2011a), but with different coefficients in the last parcel of the first member (the parcel involving $3/2$-$2n$ in equation (51) involved 1-n in the mentioned study). Appendix 1 shows the steps followed to obtain this equation. Numerical solutions were obtained using Runge-Kutta schemes of third, fourth and fifth orders. Schulz et al. (2011a) presented a first evaluation of the n profile using a fourth order Runge-Kutta method and comparing the predictions with the measured data of Janzen (2006). An improved solution was proposed by Schulz et al. (2011b) using a third order Runge-Kutta method, in which a good superposition between predictions and measurements was obtained. In the present chapter, results of the third, fourth and fifth orders approximations are shown. The system of equations derived from (51) and solved with Runge-Kutta methods is given by:

$$\begin{cases}
\dfrac{dn}{dz^*}=j, \quad \dfrac{dj}{dz^*}=w, \quad \dfrac{dw}{dy}=\dfrac{f_1+f_2}{f_3} \qquad \textit{where}\\
f_1=-A\left\{-\left[2An(1-n)+\dfrac{(1-2n)}{2}\right]w+\kappa(1-n)\left[\dfrac{2n(A-1)+1}{2}\right]+\dfrac{\left\{1+2A\left[A(1-2n)-1\right]\right\}}{A}j^2\right\}w,\\
f_2=-\kappa\left\{(A-1)(1-n)-A\left[A(1-2n)-\left(\dfrac{3}{2}-2n\right)\right]\right\}j^2,\\
\textit{and}\\
f_3=A\left[2An(1-n)+\dfrac{(1-2n)}{2}\right]j.
\end{cases} \tag{53}$$

Equations (53) were solved as an initial value problem, that is, with the boundary conditions expressed at z^*=0. In this case, $n(0)$=1 and $j(0)$=~-3 (considering the experimental data of Janzen, 2006). The value of $w(0)$ was calculated iteratively, obeying the boundary condition $0<n(1)<0.01$. The Runge-Kutta method is explicit, but iterative procedures were used to

evaluate the parameters at z^*=0 applying the quasi-Newton method and the Solver device of the Excel® table. Appendix 2 explains the procedures followed in the table. The curves of figure 6a were obtained for $0.001 \le \kappa \le 0.005$, a range based on the κ experimental values of Janzen (2006), for which ~0.003<κ<~0.004. The values A=0.5 and $n''(0)$=3.056 were used to calculate n in this figure. As can be seen, even using a constant A, the calculated curve $n(z^*)$ closely follows the form of the measured curve. Because it is known that α_f is a function of z^*, more complete solutions must consider this dependence. The curve of Schulz et al. (2011a) in figure 6a was obtained following different procedures as those described here. The curves obtained in the present study show better agreement than the former one.

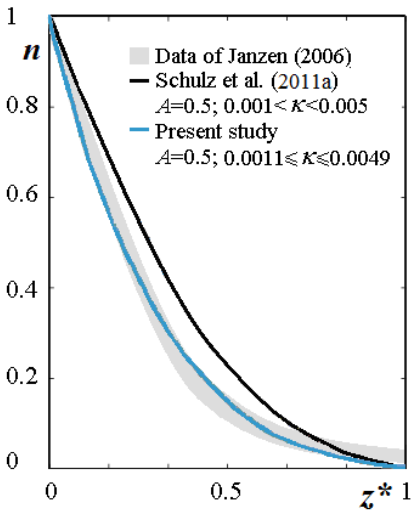

Fig. 6a. Predictions of n for $n''(0)$ = 3.056. Fourth order Runge-Kutta.

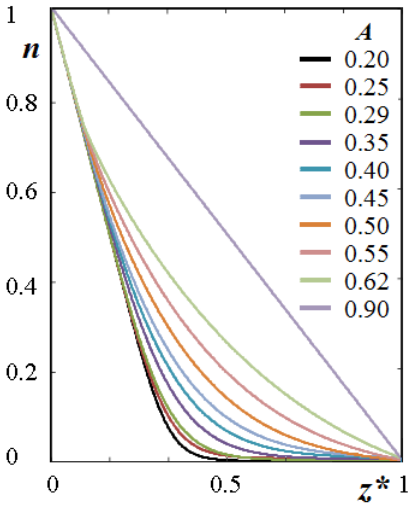

Fig. 6b. Predictions of n for κ = 0.0025, and -0.0449 ≤$n''(0)$ ≤ 3.055. Fifth order Runge-Kutta

Fig. 6b. was obtained with following conditions for the pairs [A, $n''(0)$]: [0.2, 0.00596], [0.25, -0.0145], [0.29, -0.04495], [0.35, 1.508], [0.4, 1.8996], [0.45, 1.849], [0.5, 2.509], [0.55, 3.0547], [0.62, 2.9915], [0.90, 0.00125]. Further, $n'(0)$ = -3 for A between 0.20 and 0.62, and $n'(0)$ = -1 for A=0.90.

Figure 7a shows results for κ~0.4, that is, having a value around 100 times higher than those of the experimental range of Janzen (2006), showing that the method allows to study phenomena subjected to different turbulence levels. $\kappa = (K_f E^2/D_f)$ is dependent on the turbulence level, through the parameters E and K_f, and different values of these variables allow to test the effect of different turbulence conditions on n. Figure 7b presents results similar to those of figure 6a, but using a third order Runge-Kutta method, showing that simpler schemes can be used to obtain adequate results.

As the definitions of item 3 are independent of the nature of the governing differential equations, it is expected that the present procedures are useful for different phenomena governed by statistical differential equations. In the next section, the first steps for an application in velocity-velocity interactions are presented.

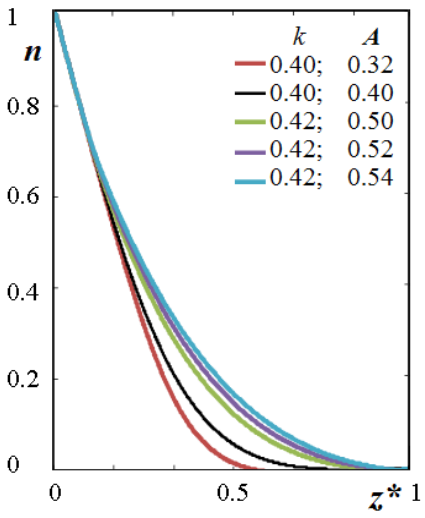

Fig. 7a. Predictions of n for $n''(0) = 3.056$, and $\kappa \sim 0.40$. Fourth order Runge-Kutta.

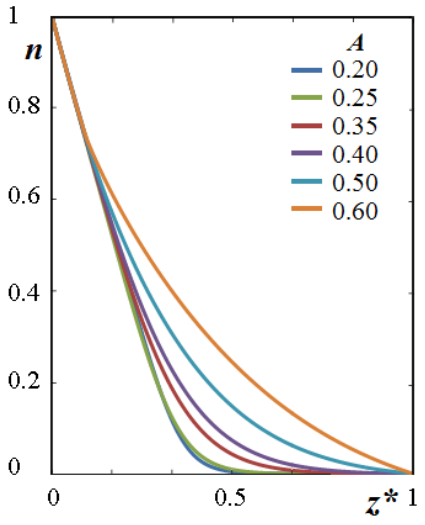

Fig. 7b. Predictions of n for $\kappa=0.003$ and $2.99812 \leq n''(0) \leq 3.2111$. Third order Runge-Kutta

3. Velocity-velocity interactions

The aim of this section is to present some first correlations for a simple velocity field. In this case, the flow between two parallel plates is considered. We follow a procedure similar to that presented by Schulz & Janzen (2009), in which the measured functional form of the reduction function is shown. As a basis for the analogy, some governing equations are first presented. The Navier-Stokes equations describe the movement of fluids and, when used to quantify turbulent movements, they are usually rewritten as the Reynolds equations:

$$\frac{\partial \overline{V}_j}{\partial t} + \overline{V}_i \frac{\partial \overline{V}_j}{\partial x_i} = \frac{\partial}{\partial x_i}\left(\upsilon \frac{\partial \overline{V}_j}{\partial x_i} - \overline{v_i v_j} \right) - \frac{1}{\rho}\frac{\partial \overline{p}}{\partial x_j} + B_i \,, \qquad \text{i, j = 1, 2, 3.} \tag{54}$$

$\overline{p}$ is the mean pressure, υ is the kinematic viscosity of the fluid and B_i is the body force per unit mass (acceleration of the gravity). For stationary one-dimensional horizontal flows between two parallel plates, equation (1), with $x_1=x$, $x_3=z$, $v_1=u$ and $v_3=\omega$, is simplified to:

$$\frac{1}{\rho}\frac{\partial \overline{p}}{\partial x} = \frac{\partial}{\partial z}\left(\upsilon \frac{\partial \overline{U}}{\partial z} - \overline{\omega u} \right) \tag{55}$$

This equation is similar to equation (2) for one dimensional scalar fields. As for the scalar case, the mean product $\overline{\omega u}$ appears as a new variable, in addition to the mean velocity $\overline{U}$. In this chapter, no additional governing equation is presented, because the main objective is to expose the analogy. The observed similarity between the equations suggests also to use the partition, reduction and superposition functions for this velocity field.

Both the upper and the lower parts of the flow sketched in figure 8 may be considered. We consider here the lower part, so that it is possible to define a zero velocity (U_n) at the lower surface of the flow, and a "virtual" maximum velocity (U_p) in the center of the flow. This virtual value is constant and is at least higher or equal to the largest fluctuations (see figure 8), allowing to follow the analogy with the previous scalar case.

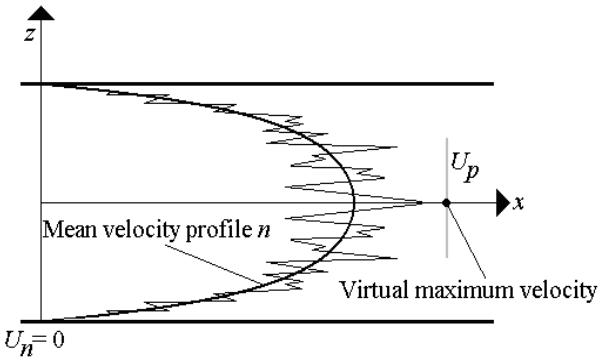

Fig. 8. The flow between two parallel planes, showing the reference velocities U_n and U_p.

The partition function n_v, for the longitudinal component of the velocity, is defined as:

$$n_v = \frac{t \text{ at } (U_p - P)}{\Delta t \text{ of the observation}} \tag{56}$$

It follows that:

$$1 - n_v = \frac{t \text{ at } (U_n + N)}{\Delta t \text{ of the observation}} \tag{57}$$

Equation (7) must be used to reduce the velocity amplitudes around the same mean velocity. It implies that the same mass is subjected to the velocity corrections P and N. As for the scalar functions, the partition function n_v is then also represented by the normalized mean velocity profile:

$$n_v = \frac{\bar{U} - U_n}{U_p - U_n} \tag{58}$$

To quantify the reduction of the amplitudes of the longitudinal velocity fluctuations, a reduction coefficient function α_u is now defined, leading, similarly to the scalar fluctuations, to:

$$\left.\begin{aligned} N &= \alpha_u n_v \left(U_p - U_n\right) \\ P &= \alpha_u \left(1 - n_v\right)\left(U_p - U_n\right) \end{aligned}\right\} \qquad 0 \le \alpha_u \le 1 \tag{59}$$

It follows, for the x components, that:

$$u_1 = (1 - n_v)\left(U_p - U_n\right)(1 - \alpha_u) \qquad \text{(positive)} \tag{60}$$

$$u_2 = -n_v\left(U_p - U_n\right)\left(1-\alpha_u\right) \qquad \text{(negative)} \tag{61}$$

The second order central moment for the x component of the velocity fluctuations is given by:

$$\overline{u^2} = {u_1}^2 n_v + {u_2}^2\left(1-n_v\right) = n_v\left(1-n_v\right)\left(1-\alpha_u\right)^2\left(U_p - U_n\right)^2 \tag{62}$$

Or, normalizing the RMS value (u'_2):

$$u'_2 = \frac{\sqrt{\overline{u^2}}}{\left(U_p - U_n\right)} = \sqrt{n_v\left(1-n_v\right)}\left(1-\alpha_u\right) \tag{63}$$

Equation 63 shows that the relative turbulence intensity profile is obtained from the mean velocity profile n_v and the reduction coefficient profile α_u. As done by Schulz & Janzen (2009), the profile of α_u can be obtained from experimental data, using equation (63).

$$1-\alpha_u = \frac{\sqrt{\overline{u^2}}}{\left(U_p - U_n\right)\sqrt{n_v\left(1-n_v\right)}} \tag{64}$$

As can be seen, the functional form of α_u is obtainable from usual measured data, with exception of the proportionality constant given by $1/U_p$, which must be adjusted or conveniently evaluated. Figure 9 shows data adapted from Wei & Willmarth (1989), cited by Pope (2000), and the function $\sqrt{n_v\left(1-n_v\right)}$ is calculated from the linear and log-law profiles close to the wall, also measured by Wei & Wilmarth (1989).

To obtain a first evaluation of the virtual constant velocity U_p, the following procedure was adopted. The value of the maximum normalized mean velocity is U/u^*~24.2 (measured), where U is the mean velocity and u^* is the shear velocity. The value of the normalized RMS u velocity, close to the peak of U, is u'/u^*~1.14. Considering a Gaussian distribution, 99.7% of the measured values are within the range fom U/u^*-3 u'/u^*. to U/u^*+3 u'/u^*. A first value of U_p is then given by U+3u', furnishing U_p/u^*~24.2+3*1.14~27.6. Physically it implies that patches of fluid with U_p are "transported" and reduce their velocity while approaching the wall. With this approximation, the partition function is given by:

$$n_v = \frac{u^+}{27.6} = \frac{\dfrac{1}{0.41}\ln y^+ + 5.2}{27.6} \tag{65}$$

The value 0.41 is the von Karman constant and the value 5.2 is adjusted from the experimental data. The notation u^+ and y^+ corresponds to the nondimensional velocity and distance, respectively, used for wall flows. In this case, $u^+=U/u^*$ and $y^+=zu^*/\nu$, where ν is the kinematic viscosity of the fluid. Equation (65) is the well-known logarithmic law for the velocity close to surfaces. It is generally applied for y^+>~11. For 0<y^+<~11, the linear form $u^+=y^+$ is valid so that equation (65) is then replaced by a linear equation between n_v and y^+. From equation (63) it follows that:

$$\frac{\sqrt{\overline{u^2}}}{u^*} = \frac{U_p}{u^*}\sqrt{n_v\left(1-n_v\right)}\left(1-\alpha_u\right) = 27.6\sqrt{n_v\left(1-n_v\right)}\left(1-\alpha_u\right) \tag{66}$$

Figure 9 shows the measured u'_2 values together with the curve given by $27.6\sqrt{n_v(1-n_v)}$. As can be seen, the curve $27.6\sqrt{n_v(1-n_v)}$ leads to a peak close to the wall. In this case, the function is normalized using the friction velocity, so that the peak is not limited by the value of 0.5 (which is the case if the function is normalized using U_p-U_n). It is interesting that the forms of $\sqrt{\overline{u^2}}/u*$ and $27.6\sqrt{n_v(1-n_v)}$ are similar, which coincides with the conclusions of Janzen (2006) for mass transfer, using *ad hoc* profiles for the mean mass concentration close to interfaces.

Figure 10 shows the cloud of points for 1-α_u obtained from the data of Wei & Willmarth (1989), following the procedures of Janzen (2006) and Schulz & Janzen (2009) for mass transfer. As for the case of mass transfer, α_u presents a minimum peak in the region of the boundary layer (maximum peak for 1-α_u).

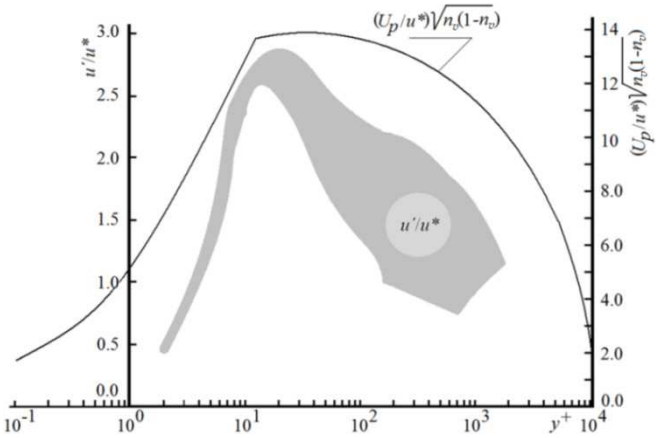

Fig. 9. Comparison between measured values of $u'/u*$ and $\left(U_p/u*\right)\sqrt{n_v(1-n_v)}$. The gray cloud envelopes the data from Wei & Willmarth (1989).

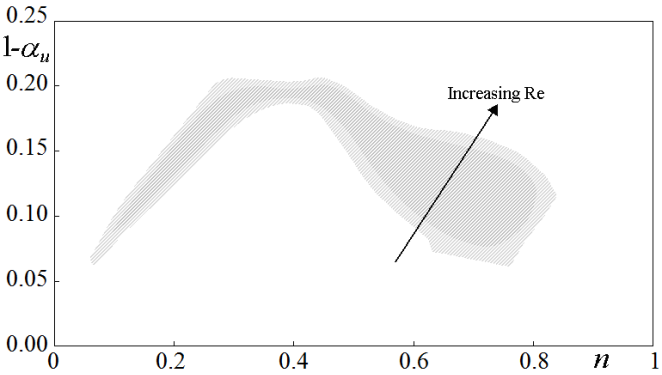

Fig. 10. 1-α_u plotted against n, following the procedures of Schulz & Janzen (2009). The gray cloud envelopes the points calculated using the data of Wei & Willmarth (1989).

As a last observation, the conclusion of section 2.7, valid for the scalar-velocity interactions, are now also valid for the transversal component of the velocity. The mean transversal velocity is null along all the flow, leading to the use of the RMS velocity for this component.

4. Challenges

After having presented the one-dimensional results for turbulent scalar transfer using the approximation of random square waves, some brief comments are made here, about some characteristics of this approximation, and about open questions, which may be considered in future studies.

As a general comment, it may be interesting to remember that the mean functions of the statistical variables are continuous, and that, in the present approximation they are defined using discrete values of the relevant variables. As described along the paper, the defined functions (n, α, β, RMS) "adjust" these two points of view (this is perhaps more clearly explained when defining the function α). This concomitant dual form of treating the random transport did not lead to major problems in the present application. Eventual applications in 2-D, 3-D problems or in phenomena that deal with discrete variables may need more refined definitions.

In the present study, the example of mass transfer was calculated by using constant reduction coefficients (α), presenting a more detailed and improved version of the study of Schulz et al. (2011a). However, it is known that this coefficient varies along z, which may introduce difficulties to obtain a solution for n. This more complete result is still not available.

It was assumed, as usual in turbulence problems, that the lower statistical parameters (e.g. moments) are appropriate (sufficient) to describe the transport phenomena. So, the finite set of equations presented here was built using the lower order statistical parameters. However, although only a finite set of equations is needed, this set may also use higher order statistics. In fact, the number of possible sets is still "infinite", because the unlimited number of statistical parameters and related equations still exists. A challenge for future studies may be to verify if the lower order terms are really sufficient to obtain the expected predictions, and if the influence of the higher order terms alter the obtained predictions. It is still not possible to infer any behavior (for example, similar results or anomalous behavior) for solutions obtained using higher order terms, because no studies were directed to answer such questions.

In the present example, only the records of the scalar variable F and the velocity V were "modeled" through square waves. It may eventually be useful for some problems also to "model" the derivatives of the records (in time or space). The use of such "secondary records", obtained from the original signal, was still not considered in this methodology.

The problem considered in this chapter was one-dimensional. The number of basic functions for two and three dimensional problems grows substantially. How to generate and solve the best set of equations for the 2-D and 3-D situations is still unknown.

Considering the above comments, it is clear that more studies are welcomed, intending to verify the potentialities of this methodology.

5. Conclusions

It was shown that the methodology of random square waves allows to obtain a closed set of equations for one-dimensional turbulent transfer problems. The methodology adopts *a priori* models for the records of the oscillatory variables, defining convenient functions that allow to "adjust" the records and to obtain predictions of the mean profiles. This is an alternative procedure in relation to the *a posteriori* "closures" generally based on *ad hoc* models, like the

use of turbulent diffusivities/viscosities, together with physical/phenomenological reasoning about relevant parameters to be considered in these diffusivities/viscosities. The basic functions are: the partition functions, the reduction coefficients and the superposition coefficients. The obtained transformed equations for the one-dimensional turbulent transport allow to obtain predictions of these functions.
In addition, the RMS of the velocity was also used as a basic function. The equations are nonlinear. An improved analysis of the one-dimensional scalar transfer through air-water interfaces was presented, leading to mean curves that superpose well with measured mean concentration curves for gas transfer. In this analysis, different constant values were used for α, κ and the second derivative at the interface, allowing to obtain well behaved and realistic mean profiles. Using the constant α values, the system of equations for one-dimensional scalar turbulent transport could be reduced to only one equation for n; in this case, a third order differential equation. In the sequence, a first application of the methodology to velocity fields was made, following the same procedures already presented in the literature for mass concentration fields. The form of the reduction coefficient function for the velocity fluctuations was calculated from measured data found in the literature, and plotted as a function of n, generating a cloud of points. As for the case of mass transfer, α_u presents a minimum peak in the region of the boundary layer (maximum peak for 1-α_u).
Because this methodology considers *a priori* definitions, applied to the records of the random parameters, it may be used for different phenomena in which random behaviors are observed.

6. Acknowledgements

The first author thanks: 1) Profs. Rivadavia Wollstein and Beate Frank (Universidade Regional de Blumenau), and Prof. Nicanor Poffo, (Conjunto Educacional Pedro II, Blumenau), for relevant advises and 2) "Associação dos Amigos da FURB", for financial support.

7. Appendix I: Obtaining equation (51)

The starting point is the set of equations (45), (46), and the definition (47).
The "*" was dropped from z^* and IJ^* in order to simplify the representation of the equations.
The main equation (45) (or 50a) then is written as

$$(1-n) = S\frac{d^2n}{dz^2} - \frac{d(IJ)}{dz} \tag{AI-1}$$

Equation (46), for θ=2, is presented as:

$$\begin{aligned} &-K_f\, n(1-n)\left(1-\alpha_f\right)^2 + \sqrt{\frac{\left[n(1-n)\right]}{n(1-n)+\dfrac{\beta(1-\beta)}{(2\beta-1)^2}}}\left[n(1-n)\right]^{1/2}\sqrt{\overline{\omega^2}}\left(1-\alpha_f\right)\frac{\partial n}{\partial z} + \\ &+\frac{1}{2}\frac{\partial}{\partial z}\left\{\sqrt{\frac{1}{n(1-n)+\dfrac{\beta(1-\beta)}{(2\beta-1)^2}}}\left[(1-2n)\right]\left[n(1-n)\left(1-\alpha_f\right)^2\right]\sqrt{\overline{\omega^2}}\right\} = \\ &= D_f\left\{\frac{\partial^2\left[(1-n)(1-\alpha_c)\right]}{\partial z^2} + \frac{\partial^2\left[-n(1-\alpha_c)\right]}{\partial z^2}\right\} n(1-n)\left(1-\alpha_f\right) \end{aligned} \tag{AI-2}$$

Using the definitions $IJ = \dfrac{n(1-n)(1-\alpha_f)\dfrac{\sqrt{\overline{\omega^2}}}{Ke}}{\sqrt{n(1-n)+\dfrac{\beta(1-\beta)}{(2\beta-1)^2}}}$ and $S = \dfrac{D}{Ke^2}$:

$$\begin{aligned} &-n(1-n)(1-\alpha_c)^2 + IJ\frac{\partial n}{\partial z} + \frac{1}{2}\frac{\partial}{\partial z}\left\{(1-2n)(1-\alpha_c)IJ\right\} = \\ &= S\left\{\frac{\partial^2\left[(1-n)(1-\alpha_c)\right]}{\partial z^2} + \frac{\partial^2\left[-n(1-\alpha_c)\right]}{\partial z^2}\right\} n(1-n)(1-\alpha_c) \end{aligned} \tag{AI-3}$$

For α_f constant and defining A=(1 − α_f):

$$-n(1-n)A^2 + IJ\frac{dn}{dz} - IJA\frac{dn}{dz} + \frac{(1-2n)}{2}A\frac{dIJ}{dz} = -2S\left\{\frac{d^2n}{dz^2}\right\} n(1-n)A^2 \tag{AI-4}$$

Using equations (AI1) and (AI4)

$$\begin{aligned} -n(1-n)A^2 - \frac{(1-n)(1-2n)}{2}A + IJ(1-A)\frac{dn}{dz} = \\ = -2S\left\{\frac{d^2n}{dz^2}\right\} n(1-n)A^2 - S\frac{(1-2n)}{2}A\left\{\frac{d^2n}{dz^2}\right\} \end{aligned} \tag{AI-5}$$

Solving equation (AI5) for *IJ*:

$$IJ = \frac{-2S\left\{\dfrac{d^2n}{dz^2}\right\} n(1-n)A^2 - S\dfrac{(1-2n)}{2}A\left\{\dfrac{d^2n}{dz^2}\right\} + n(1-n)A^2 + \dfrac{(1-n)(1-2n)}{2}A}{(1-A)\dfrac{dn}{dz}} \tag{AI-6}$$

Rearranging equation (AI6):

$$\frac{(1-A)}{A}IJ = \frac{-S\left\{2An(1-n) + \dfrac{(1-2n)}{2}\right\}\left\{\dfrac{d^2n}{dz^2}\right\} + (1-n)\left[\dfrac{2n(A-1)+1}{2}\right]}{\dfrac{dn}{dz}} \tag{AI-7}$$

Differentiating equation (AI7) and using equation (AI1):

$$\begin{aligned} &\frac{(1-A)}{A}\left[S\frac{d^2n}{dz^2} - (1-n)\right] = \\ &= \frac{-S\left\{2A\left[\dfrac{dn}{dz} - 2n\dfrac{dn}{dz}\right] - \dfrac{dn}{dz}\right\}\left\{\dfrac{d^2n}{dz^2}\right\} - S\left\{2An(1-n) + \dfrac{(1-2n)}{2}\right\}\left\{\dfrac{d^3n}{dz^3}\right\} +}{\dfrac{dn}{dz}} \end{aligned}$$

$$+\frac{\left(-\frac{dn}{dz}\right)\left[\frac{2n(A-1)+1}{2}\right]+(1-n)\left[\frac{(A-1)dn}{dz}\right]}{\frac{dn}{dz}}-$$
$$-\frac{-S\left\{2An(1-n)+\frac{(1-2n)}{2}\right\}\left\{\frac{d^2n}{dz^2}\right\}+(1-n)\left[\frac{2n(A-1)+1}{2}\right]}{\left(\frac{dn}{dz}\right)^2}\left\{\frac{d^2n}{dz^2}\right\} \quad \text{(AI-8)}$$

Multiplying by $\left(\frac{dn}{dz}\right)^2$ and simplifying $\frac{dn}{dz}$:

$$\frac{(1-A)}{A}\left[S\frac{d^2n}{dz^2}-(1-n)\right]\left(\frac{dn}{dz}\right)^2=$$
$$=-\left(\frac{dn}{dz}\right)^2 S\left\{2A[1-2n]-1\right\}\left\{\frac{d^2n}{dz^2}\right\}-$$
$$-\left(\frac{dn}{dz}\right)S\left\{2An(1-n)+\frac{(1-2n)}{2}\right\}\left\{\frac{d^3n}{dz^3}\right\}+ \quad \text{(AI-9)}$$
$$+\left(\frac{dn}{dz}\right)^2\left\{-\left[\frac{2n(A-1)+1}{2}\right]+(1-n)(A-1)\right\}-$$
$$-\left\{-S\left\{2An(1-n)+\frac{(1-2n)}{2}\right\}\left\{\frac{d^2n}{dz^2}\right\}+(1-n)\left[\frac{2n(A-1)+1}{2}\right]\right\}\left\{\frac{d^2n}{dz^2}\right\}$$

Rearranging (after multiplying the equation by A and using $S=1/\kappa$):

$$A\left[2An(1-n)+\frac{(1-2n)}{2}\right]\frac{d^3n}{dz^3}\frac{dn}{dz}+$$
$$+A\left\{\begin{array}{l}-\left[2An(1-n)+\frac{(1-2n)}{2}\right]\frac{d^2n}{dz^2}+\kappa(1-n)\left[\frac{2n(A-1)+1}{2}\right]+\\ +\frac{\left\{1+2A\left[A(1-2n)-1\right]\right\}}{A}\left(\frac{dn}{dz}\right)^2\end{array}\right\}\frac{d^2n}{dz^2}+ \quad \text{(AI-10)}$$
$$+\kappa\left\{(A-1)(1-n)-A\left[A(1-2n)-\left(\frac{3}{2}-2n\right)\right]\right\}\left(\frac{dn}{dz}\right)^2$$
$$=0$$

Equation (AI10) is the equation (51) presented in the text.

8. Appendix II: Solving equation (51) using mathematical tables

Equation (51) (or equation (AI-10)) of this chapter is a third order nonlinear ordinary differential equation, for which adequate numerical methods must be applied. Some methods were considered to solve it.

A first attempt was made using the second order Finite Differences Method and the solver device from the Microsoft Excel® table, intending to solve the problem with simple and practical tools, but the results were not satisfactory. It does not imply that the Finite Differences Method does not apply, but only that we wanted more direct ways to check the applicability of equation (51).
The second attempt was made using Runge-Kutta methods, also furnished in mathematical tables like Excel ®, maintaining the objective of solving the one-dimensional problem with simple tools. In this case, the results were adequate, superposing well the experimental data.
The Runge-Kutta methods were developed for ordinary differential equations (ODEs) or systems of ODEs. Equation (AI-10) is a nonlinear differential equation, so that it was necessary to first rewrite it as a system of ODEs, as follows

$$\frac{dn}{dz} = j \tag{AII-1}$$

$$\frac{d^2n}{dz^2} = w \tag{AII-2}$$

$$\frac{dw}{dz} = (f_1 + f_2) / f_3 \tag{AII-3}$$

in which

$$f_1 = -A\left\{\begin{array}{l} -\left[2An(1-n)+\dfrac{(1-2n)}{2}\right]w+\kappa(1-n)\left[\dfrac{2n(A-1)+1}{2}\right]+ \\ +\dfrac{\{1+2A[A(1-2n)-1]\}}{A}j^2 \end{array}\right\}w \tag{AII-4}$$

$$f_2 = -\kappa\left\{(A-1)(1-n)-A\left[A(1-2n)-\left(\frac{3}{2}-2n\right)\right]\right\}j^2 \tag{AII-5}$$

$$f_3 = A\left[2An(1-n)+\frac{(1-2n)}{2}\right]j \tag{AII-6}$$

Figure 6 shows that 3th, 4th and 5th orders Runge-Kutta methods were applied to obtain numerical results for the profile of n. This Appendix shows a summary of the use of the 5th order method. Of course, similar procedures were followed for the lower orders. As usual in this chapter, equations (AII-1) up to (AII-3) use the nondimensional variable z without the star "*" (that is, it corresponds to z^*). Considering "y" the dependent variable in a given ODE, the of 5th order method, presented by Butcher (1964) appud Chapra and Canale (2006), is written as follows

$$y_{k+1} = y_k + \frac{\Delta x}{90}(7\psi_1 + 32\psi_3 + 12\psi_4 + 32\psi_5 + 7\psi_6) \tag{AII-7}$$

in which

$$\begin{cases} \psi_1 = f\left(x_k, y_k\right) \\ \psi_2 = f\left(x_k + \frac{1}{4}\Delta x, y_k + \frac{1}{4}\psi_1 \Delta x\right) \\ \psi_3 = f\left(x_k + \frac{1}{4}\Delta x, y_k + \frac{1}{8}\psi_1 \Delta x + \frac{1}{8}\psi_2 \Delta x\right) \\ \psi_4 = f\left(x_k + \frac{1}{2}\Delta x, y_k - \frac{1}{2}\psi_2 \Delta x + \psi_3 \Delta x\right) \\ \psi_5 = f\left(x_k + \frac{3}{4}\Delta x, y_k + \frac{3}{16}\psi_1 \Delta x + \frac{9}{16}\psi_4 \Delta x\right) \\ \psi_6 = f\left(x_k + \Delta x, y_k - \frac{3}{7}\psi_1 \Delta x + \frac{2}{7}\psi_2 \Delta x + \frac{12}{7}\psi_3 \Delta x - \frac{12}{7}\psi_4 \Delta x + \frac{8}{7}\psi_5 \Delta x\right) \end{cases} \quad \text{(AII-8)}$$

In the system of equations (AII-8), generated from equations (AII-4) through (AII-6), $x = z$ and $y = n$, following the representation used in this chapter.

The system of equations (AII-1) through (AII-6) was solved using a spreadsheet for Microsoft Excel®, available at www.stoa.usp.br/hidraulica/files/. Two initial values were fixed and one was calculated. Note that in the present study it was intended to verify if the method furnishes a viable profile, so that boundary or initial values obtained from the experimental data were assumed as adequate. The first was $n(0)=1$. The second was $n'(0)=-3$, corresponding to the experiments of Janzen (2006). The third information did not constitute an initial value, and was $n(1)=0$ or $0<n(1)<0.01$ (threshold value corresponding to the definition of the boundary layer). As the Runge-Kutta methods need initial values, this information was used to obtain $n''(0)$, the remaining initial value needed to perform the calculations. With the aid of the Newton (or quasi-Newton) method, it was possible to obtain values for $n''(0)$ that satisfied the third condition imposed at $z = 1$.

The derivative of n at $z=0$ is generally unknown in such mass transfer problems. In this case, solutions must be found considering, for example, $n(0)=1$, $0<n(1)<0.01$ and $n'(1)=0$ (three reasonable boundary conditions), for which another scheme must be developed to calculate the first and second derivatives at the origin. As mentioned, the aim of this study was to verify the applicability of the method. The details of solutions for different purposes must be considered by the researchers interested in that solution.

The construction of the spreadsheet is described in the following steps:

i. determine the initial values: $n(0) = 1$, $n'(0) = -3$ (or other appropriate value) $n''(0)$ = initial guess;
ii. Compute $\psi_{1,1}$ and $\psi_{1,2}$, the function values f_1, f_2 e f_3 with the initial values, and then $\psi_{1,3}$. In the variable $\psi_{i,j}$, i = 1,2,...,6 and j = 1,2,3, the first index corresponds to the six stages of the method and the second to the order of the ODE that generated the original system to be solved;
iii. With the values calculated in (ii), calculate now $n_k+(1/4)\,\psi_{1,1}\,\Delta z$, $j_k+(1/4)\,\psi_{1,1}\,\Delta z$ and $w_k+(1/4)\,\psi_{1,1}\,\Delta z$. The following steps are similar until $j = 6$;
iv. Equation AII-7 (a system) is then used to advance in space z.

The spreadsheet available at www.stoa.usp.br/hidraulica/files/ presents some suggestions that simplify some items of the above described steps (some manual work is simplified). The estimate of n"(0), for example, is obtained following simplified procedures.

9. References

Brodkey, R.S. (1967) The phenomena of Fluid Motions, *Addison–Wesley Publishing Company*, Reading, Massachusetts.

Butcher, J.C. (1964). On Runge-Kutta methods of high order. J.Austral. Math. Soc.4, p.179-194.

Chapra, S.C.; Canale, R.P. (2006). Numerical methods for engineers. McGraw-Hill, 5th ed., 926 p.

Corrsin, S. (1957) Simple theory of an idealized turbulent mixer, AIChE J., 3(3), pp. 329-330.

Corrsin, S. (1964) The isotropic turbulent mixer: part II - arbitrary Schmidt number, AIChE J., 10(6), pp. 870-877.

Donelan, M.A., Drennan, W.M., Saltzman, E.S. & Wanninkhof, R. (2002) Gas Transfer at Water Surfaces, Geophysical Monograph Series, American Geophysical Union, Washington, U.S.A., 383 p.

Hinze, J.O. (1959), Turbulence, Mc. Graw-Hill Book Company, USA, 586 p.

Jähne, B. & Monahan, E.C. (1995) Air-Water Gas Transfer, Selected papers from the Third International Symposium on Air-Water Gas Transfer, Heidelberg, Germany, AEON Verlag & Studio, 918 p.

Janzen, J.G. (2006) Fluxo de massa na interface ar-água em tanques de grades oscilantes e detalhes de escoamentos turbulentos isotrópicos (Gas transfer near the air-water interface in an oscillating-grid tanks and properties of isotropic turbulent flows – text in Portuguese). Doctoral thesis, University of Sao Paulo, São Carlos, Brazil.

Janzen, J.G., Herlina,H., Jirka, G.H., Schulz, H.E. & Gulliver, J.S. (2010), Estimation of Mass Transfer Velocity based on Measured Turbulence Parameters, AIChE Journal, V.56, N.8, pp. 2005-2017.

Janzen J.G, Schulz H.E. & Jirka GH. (2006) Air-water gas transfer details (portuguese). Revista Brasileira de Recursos Hídricos; 11, pp. 153-161.

Janzen, J.G., Schulz, H.E. & Jirka, G.H. (2011) Turbulent Gas Flux Measurements near the Air-Water Interface in an Oscillating-Grid Tank. In Komori, S; McGillis, W. & Kurose, R. Gas Transfer at Water Surfaces 2010, Kyoto University Press, Kyoto, pp. 65-77.

Monin, A.S. & Yaglom, A.M. (1979), Statistical Fluid Mechanics: Mechanics of Turbulence, Volume 1, the MIT Press, 4th ed., 769p.

Monin, A.S. & Yaglom, A.M. (1981), Statistical Fluid Mechanics: Mechanics of Turbulence, Volume 2, the MIT Press, 2th ed., 873p.

Pope, S.B. (2000), Turbulent Flows, Cambridge University Press, 1st ed., UK, 771p.

Schulz, H.E. (1985) Investigação do mecanismo de reoxigenação da água em escoamento e sua correlação com o nível de turbulência junto à superfície - 1. (Investigation of the roxigenation mechanism in flowing waters and its relation to the turbulence level at the surface-1 – text in Portuguese) MSc dissertation, University of São Paulo, Brazil São Carlos. 299p.

Schulz, H.E.; Bicudo, J.R., Barbosa, A.R. & Giorgetti, M.F. (1991) Turbulent Water Aeration: Analytical Approach and Experimental Data, In Wilhelms, S.C. and Gulliver, J.S., eds. Air Water Mass Transfer, ASCE, New York, pp.142-155.

Schulz, H.E. & Janzen, J.G. (2009) Concentration fields near air-water interfaces during interfacial mass transport: oxygen transport and random square wave analysis. *Braz. J. Chem. Eng.* vol.26, n.3, pp. 527-536.

Schulz, H.E., Lopes Junior, G.B. & Simões, A.L.A. (2011b) Gas-liquid mass transfer in turbulent boundary layers using random square waves, 3rd workshop on fluids

and PDE, June 27 to July 1, Institute of Mathematics, Statistics and Scientific Computation, Campinas, Brazil.

Schulz H.E. & Schulz S.A.G. (1991) Modelling below-surface characteristics in water reaeration. Water pollution, modelling, measuring and prediction. Computational Mechanics Publications and Elsevier Applied Science, pp. 441–454.

Schulz, H.E., Simões, A.L.A. & Janzen, J.G. (2011a), Statistical Approximations in Gas-Liquid Mass Transfer, In Komori, S; McGillis, W. & Kurose, R. Gas Transfer at Water Surfaces 2010, Kyoto University Press, Kyoto, pp. 208-221.

Wilhelms, S.C. & Gulliver, J.S. (1991) Air-Water Mass Transfer, Selected Papers from the Second International Symposium on Gas Transfer at Water Surfaces, Minneapolis, U.S.A., ASCE, 802 p.

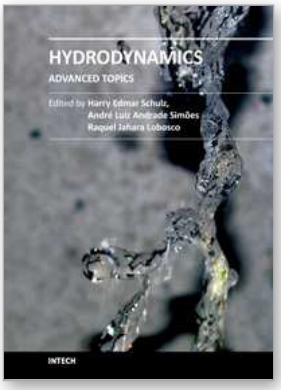

Hydrodynamics - Advanced Topics

Edited by Prof. Harry Schulz

ISBN 978-953-307-596-9
Hard cover, 442 pages
Publisher InTech
Published online 22, December, 2011
Published in print edition December, 2011

The phenomena related to the flow of fluids are generally complex, and difficult to quantify. New approaches - considering points of view still not explored - may introduce useful tools in the study of Hydrodynamics and the related transport phenomena. The details of the flows and the properties of the fluids must be considered on a very small scale perspective. Consequently, new concepts and tools are generated to better describe the fluids and their properties. This volume presents conclusions about advanced topics of calculated and observed flows. It contains eighteen chapters, organized in five sections: 1) Mathematical Models in Fluid Mechanics, 2) Biological Applications and Biohydrodynamics, 3) Detailed Experimental Analyses of Fluids and Flows, 4) Radiation-, Electro-, Magnetohydrodynamics, and Magnetorheology, 5) Special Topics on Simulations and Experimental Data. These chapters present new points of view about methods and tools used in Hydrodynamics.

InTech Europe
University Campus STeP Ri
Slavka Krautzeka 83/A
51000 Rijeka, Croatia
Phone: +385 (51) 770 447
Fax: +385 (51) 686 166
www.intechopen.com

InTech China
Unit 405, Office Block, Hotel Equatorial Shanghai
No.65, Yan An Road (West), Shanghai, 200040, China
中国上海市延安西路65号上海国际贵都大饭店办公楼405单元
Phone: +86-21-62489820
Fax: +86-21-62489821